ELSEVIER

Journal of Chromatography A, 858 (1999) 133–153

JOURNAL OF CHROMATOGRAPHY A

www.elsevier.com/locate/chroma

n-Alkyl fluorenyl phases in chromatography II. Dynamic behavior and high-performance liquid chromatography applications

Arndt Ellwanger[a], Rainer Brindle[a], Manfred Kaiser[b], Wolfram Wielandt[c], Ekkehard Lindner[c], Klaus Albert[a,*]

[a]*Institut für Organische Chemie, Auf der Morgenstelle 18, D-72076 Tübingen, Germany*
[b]*Wehrwissenschaftliches Institut für Werk-, Explosiv- und Betriebsstoffe, Grosses Cent, D-53913 Swisttal, Germany*
[c]*Institut für Anorganische Chemie, Auf der Morgenstelle 18, D-72076 Tübingen, Germany*

Received 31 August 1998; received in revised form 23 July 1999; accepted 26 July 1999

Abstract

The dynamic behavior of two *n*-hexyl fluorenyl phases (fluorene-6A [3a(T^n)(Q^m)$_y$], fluorene-6B [3b(T^n)(Q^m)$_y$]) and three *n*-decyl fluorenyl phases (fluorene-10A [4a(T^n)(Q^m)$_y$], fluorene-10B [4b(T^n)(Q^m)$_y$], and fluorene-10C [4c(M^1)(Q^m)$_y$]) is investigated by solid-state nuclear magnetic resonance (NMR) spectroscopy using the dipolar filter technique with both ^{13}C and ^1H detection. These results are compared with those from other dynamic measurements, like the relaxation times in the rotating frame ($T_{1\rho H}$) and the variation of the contact time (T_{CH}). Additionally, another type of a fluorenyl phase [5a(T^n)(Q^m)$_y$], which has an aromatic moiety connected to the silica gel by amido couplings, was also investigated by the dipolar filter method. The solid-state NMR dynamic measurements indicate an increased mobility of the *n*-alkyl fluorenyl phases compared to the amido coupled fluorenyl phase. The lower the ligand density of the studied *n*-alkyl fluorenyl phases, the higher their mobility. The separation behavior of the respective phases in high-performance liquid chromatography was investigated with samples containing polycyclic aromatic hydrocarbons and nitro explosives. Depending on the amount of the chemically bound aromatic moiety and the length of their *n*-alkyl spacer groups, π–π interactions with the solute molecules are involved in the separation process and cause it to proceed at a different rate. Therefore, *n*-alkyl fluorenyl phases can be classified as mixed-mode phases.

Keywords: Alkyl fluorenyl stationary phases; Stationary phases; LC; Fluorenyl stationary phases; Nuclear magnetic resonance spectrometry; π–π Interactions; Polynuclear aromatic hydrocarbons; Explosives; Nitro explosives

1. Introduction

For analytical issues HPLC [1,2] has become a widespread and powerful method which belongs among the basic tools in each modern laboratory nowadays. Everybody who has practical experience with HPLC knows that the optimization of a separation problem by varying parameters such as mobile phase composition, temperature, or employing a gradient is an essential but time consuming task. In some cases no satisfying separation is obtained, although many other problems were successfully

*Corresponding author. Tel.: +49-70-71-2975335; fax: +49-70-71-295875.
E-mail address: klaus.albert@uni-tuebingen.de (K. Albert)

0021-9673/99/$ – see front matter
PII: S0021-9673(99)00828-6

solved on the employed column. Replacing a column by a more suitable column for the separation problem is usually regarded as the last option. Selecting first a suitable stationary phase followed by an optimization of the other parameters helps to save much time but it requires good knowledge of the structural differences and the capabilities of the available columns. Unfortunately, this order for obtaining good resolution is often neglected, because the range and characteristics of the existing stationary phases are not generally known.

Stationary phases based on silica gel with attached C_{18} alkyl chains are most common in HPLC. C_{18} phases [1–4] are offered in countless variations with specific chromatographic properties by different manufacturers. They differ for example in parameters such as ligand density, particle and pore size of the silica gel, or the functionality of the attached C_{18} silane. Various classes of compounds have been separated by C_{18} phases, but there is still a demand for tailored stationary phases due to unresolved separation problems. One possibility is a variation of the alkyl chain length [5]. An improved selectivity for the separation of vitamin-A acetates [6] and β-carotene [7] isomers was reported for stationary phases with attached C_{30} alkyl chains [8–10]. Recently, C_{22} and C_{34} phases [5,11] were employed for the first time in HPLC as further alternatives to conventional C_{18} phases.

A completely different approach to new tailored stationary phases based on silica gel has been introduced by phases with attached aromatic moieties. Many stationary phases containing aromatic ligand fragments such as acridine, anthracene, pyrene, or fluorene have been described in the literature [12–20] already. In contrast to *n*-alkyl phases with a predominance of hydrophobic interactions [21], the π-electron systems [22,23] of the attached aromatic moieties also play an important role for those phases during the separation process. An interesting new representative of the latter type was developed [19], recently. A fluorenyl phase was designed for the separation of substances containing aromatic molecules such as polycyclic aromatic hydrocarbons or nitro explosives, which are both regarded as an obvious potential danger for the environment. The important contribution by π–π interactions [22] of the fluorene ligand fragments to the separation process was demonstrated by the inverse elution order of the nitro aromatic solute molecules with respect to a conventional C_{18} phase [24]. In the case of the described fluorenyl phase, the aromatic moiety was connected to silica gel by amido couplings with spacers of amino alkyl silanes and glutaric acid. Partial double bonds of the C–N spacer groups drastically reduce the mobility of the whole ligand system including the fluorene fragments and this could be proved by solid-state NMR spectroscopy [19]. The best chromatographic capabilities on PAH samples were observed for the phase with the highest mobility of this rather immobile amido coupled fluorenyl phase type.

Therefore, our intention was the development of a new kind of fluorenyl phases with a higher overall mobility compared to amido coupled fluorenyl phases for the separation of aromatic solutes. The higher system mobility was intended to increase the effectiveness of the fluorene ligand fragments acting as the main interaction center during the separation process. Thus, we created a combination of a fluorenyl and a *n*-alkyl phase [25,26], because the latter phase type exhibits a much higher system mobility than amido coupled aromatic phases [19,20,27].

In the first part of this paper five new *n*-alkyl fluorenyl phases for chromatography were introduced [25]. Each of those stationary phases consists of fluorene which is connected at its 9-position by either a *n*-hexyl (in the case of fluorene-6A [3a(T^n)(Q^m)$_y$] and fluorene-6B [3b(T^n)(Q^m)$_y$]) or a *n*-decyl spacer (in the case of fluorene-10A [4a(T^n)(Q^m)$_y$], fluorene-10B [4b(T^n)(Q^m)$_y$], and fluorene-10C [4c(M^1)(Q^m)$_y$]) to the silica gel surface. Depending on the silane *n*-alkyl fluorenyl phases used, different ligand densities were obtained. High ligand densities were achieved with trichloro silanes (fluorene-6A [3a(T^n)(Q^m)$_y$] and fluorene-10A [4a(T^n)(Q^m)$_y$]) in contrast to low ligand densities due to employing the respective triethoxy silanes (fluorene-6B [3b(T^n)(Q^m)$_y$] and fluorene-10B [4b(T^n)(Q^m)$_y$]). Even by the use of monochloro silane (fluorene-10C [4c(M^1)(Q^m)$_y$]) a higher ligand density was obtained as compared to phases synthesized with triethoxy silanes. The structure of the *n*-alkyl fluorenyl phases was characterized with solid-state NMR spectroscopy. Information about the

surface of the chemically modified silica gel was provided by ^{29}Si cross-polarization (CP) magic angle spinning (MAS) NMR spectroscopy, whereas information about the different organic ligand fragments was detected by both ^{13}C CP-MAS and ^{1}H-MAS-NMR spectroscopy. In the latter case a better resolution and a reduced line width of the signal of the aromatic ligand fragments indicated a higher overall mobility for *n*-alkyl fluorene phases than for amido coupled fluorenyl phases. Their utility in HPLC and the contribution of π–π interactions to the separation process was demonstrated by using the Sander and Wise test (SRM 869) [28,29].

For getting a closer insight into the dynamics of stationary phases, solid-state NMR spectroscopy [30] is the method of choice. There are several special dynamic measurement techniques to choose from. Well known ones are the variation of the contact time and the spin-lattice relaxation times in the rotating frame experiments [31,32]. Impressive alternatives to those conventional dynamic methods were developed by Spiess et al. [33]. Derived from the Goldman–Shen experiment [34] the 2D (two-dimensional) WISE (wide line separation) technique is used for the correlation of segmental mobility (^{1}H line widths) and structure (^{13}C chemical shifts) in organic solids [35,36]. Unfortunately, this powerful method is too time consuming for an application on stationary phases of the *n*-alkyl fluorenyl type. Even for phases with a high ligand density it takes at least two hours to obtain a reasonable resolved ^{13}C CP-MAS-NMR spectrum. Usually, a 2D WISE NMR spectrum is detected with a data matrix of at least 64 (experiments) in the t_1 (^{1}H) dimension, thus the time problem, especially for phases with a low ligand density, becomes clearly visible. The rather low mobility of aromatic stationary phases detected as broad ^{13}C-NMR signals has an additional negative impact on the signal-to-noise ratio.

Another, less time consuming method was also introduced by Spiess et al. This method, called the dipolar filter technique [37,38], is closely related to the 2D WISE experiment. It is well suited for the dynamic investigation of organic solids with a rather low amount of signal contributing fragments such as stationary phases containing aromatic ligand fragments. Information about the mobility can be received by 1D (one-dimensional) ^{13}C as well as ^{1}H-NMR detection. The magnetization of more mobile ligand fragments becomes separated from the magnetization of more rigid ligand fragments due to the implementation of a multiple pulse sequence. Both, the 2D WISE experiment as well as the dipolar filter technique can also be applied to the determination of domain sizes by spin diffusion in organic polymers built up of fragments with a different mobility.

In this paper, we investigate the dynamics of five *n*-alkyl fluorenyl phases and the most mobile representative of the amido coupled fluorenyl phases by solid-state NMR spectroscopy. The dipolar filter and the $T_{1\rho H}$ technique by both, ^{13}C and ^{1}H detection, as well as the variation of the contact time experiment were employed for this issue. The influence of system mobility and ligand density on the separation behavior of the respective stationary phases is investigated. The involvement of π–π interactions with the separation process and the chromatographic capabilities of the respective *n*-alkyl fluorenyl phases were determined with samples containing PAHs and nitro explosives.

2. Experimental

2.1. Synthesis and materials

The synthesis of the *n*-alkyl fluorenyl phases is thoroughly described in the first part of this paper, whereas the synthesis of the amido coupled fluorenyl phase is described elsewhere [19]. A detailed list of the employed materials for the synthesis of the stationary phases is also presented in the respective references.

The SRM 1647 (16 PAHs) standard was a gift from the National Institute of Standards and Technology (Gaithersburg, MD, USA). The individual PAHs of this sample were obtained from Supelco (Deisenhofen, Germany). The nitro explosives were donated by WIWEB (Swisttal, Germany). Acetonitrile and methanol for HPLC were of LiChrosolv gradient grade from Merck (Darmstadt, Germany).

2.2. Solid-state NMR spectroscopy

^{13}C and ^{1}H dipolar filter solid-state NMR spectra were obtained on a Bruker ASX 300 NMR spec-

trometer at 7 T. For ^{1}H-NMR measurements 4 mm rotors of ZrO_2 were spun at 14 kHz by a dry air gas drive. Recycle delay: 4 s, 90 degree pulse length: 3.6 μs, transients: 32. ^{13}C-NMR measurements were carried out with 7 mm rotors at a spinning rate of 4 kHz. Proton 90 degree pulse length: 5.0 μs, contact time: 300 μs, recycle delay: 1 s, transients: between 7000 and 18 000, depending on the ligand density. The number of transients has to be exactly the same for dipolar filter NMR spectra, differing in the waiting period, at the same stationary phase.

^{1}H $T_{1\rho H}$ NMR measurements were performed under analogous condition as described for the dipolar filter experiment. ^{13}C-CP-MAS variation of contact time and $T_{1\rho H}$ NMR experiments were obtained on a Bruker MSL 200 NMR spectrometer at 4.7 T. The measurements were carried out with 7 mm rotors at a spinning rate of 4 kHz. Proton 90 degree pulse length: 6.0 μs, contact time: 1 ms, recycle delay: 1 s, transients: between 7000 and 16 000, depending on the ligand density.

All chemical shifts were externally referenced to liquid tetramethylsilane, the Hartmann–Hahn condition for CP was calibrated with glycine.

2.3. Chromatography

HPLC separations were performed with a Merck–Hitachi L-6200 A pump in combination with a variable wavelength detector Merck–Hitachi L-4000 A (Merck–Hitachi, Darmstadt, Germany) and with a Hewlett-Packard HP Series 1100 system (Hewlett-Packard, Waldbronn, Germany). The stationary phases were packed into 250×4 mm stainless steel tubes (Bischoff, Leonberg, Germany) by a high-pressure slurry packing procedure on a Knauer Pneumatic HPLC pump (Knauer, Berlin, Germany).

The mobile phase composition for the SRM 1647 test/16 PAHs differed depending on the used *n*-alkyl fluorenyl phase. Fluorene-6A[3a(T^n)(Q^m)$_y$], gradient elution program as follows: 10 min hold at methanol–water (70:30, v/v), a 30 min linear gradient to methanol–water (90:10, v/v), and hold until the end of the separation. Fluorene-10A[4a(T^n)(Q^m)$_y$], gradient elution program as follows: a 20 min linear gradient from methanol–water (70:30, v/v) to (90:10, v/v), and hold until the end of the separation. Fluorene-10B[4b(T^n)(Q^m)$_y$]: isocratic separation with methanol–water (80:20, v/v). Fluorene-10C[4c(M^1)(Q^m)$_y$], gradient elution program as follows: 15 min hold at methanol–water (70:30, v/v), a 15 min linear gradient to methanol–water (80:20, v/v), and hold until the end of the separation. In each case a 20 μl volume of the test sample was injected.

The mobile phase composition for the nitro explosives was either methanol–water (50:50, v/v) or (40:60, v/v), and a 20 μl volume of the sample was injected containing about 5 μg/ml of each compound.

All separations were carried out with UV detection at 254 nm, 1 ml/min flow-rate and 25°C temperature.

3. Results

3.1. Investigation of the dynamic behavior by solid-state NMR spectroscopy

3.1.1. The dipolar filter technique

Information about the structure of stationary phases based on silica gel can be easily attained by conventional ^{29}Si, ^{13}C, and ^{1}H solid-state NMR experiments [5,20,25,39–44], whereas their dynamic behavior has to be investigated by separate, more complex solid-state NMR experiments. Comparing the dynamics of the different fluorenyl phases is a very interesting issue, because explanations for differences in the chromatographic capabilities of the respective phases can be provided on this way. For a better comparison about their structural differences, the investigated fluorenyl phases are depicted in Fig. 1.

The dipolar filter technique was developed by Spiess et al. [37,38] as a powerful tool for obtaining information about the dynamics of solid organic polymers. This technique is based on the Goldman–Shen experiment. Fragments which differ in their mobility can be separated by this method due to differences in their dipolar coupling strength. The separation is achieved by inserting a variable waiting time for the evolution of the proton magnetization between the exitation by a 90° pulse on the proton channel and the signal acquisition, by either ^{1}H or ^{13}C detection. The stronger the dipolar coupling strength, the faster the magnetization of the respec-

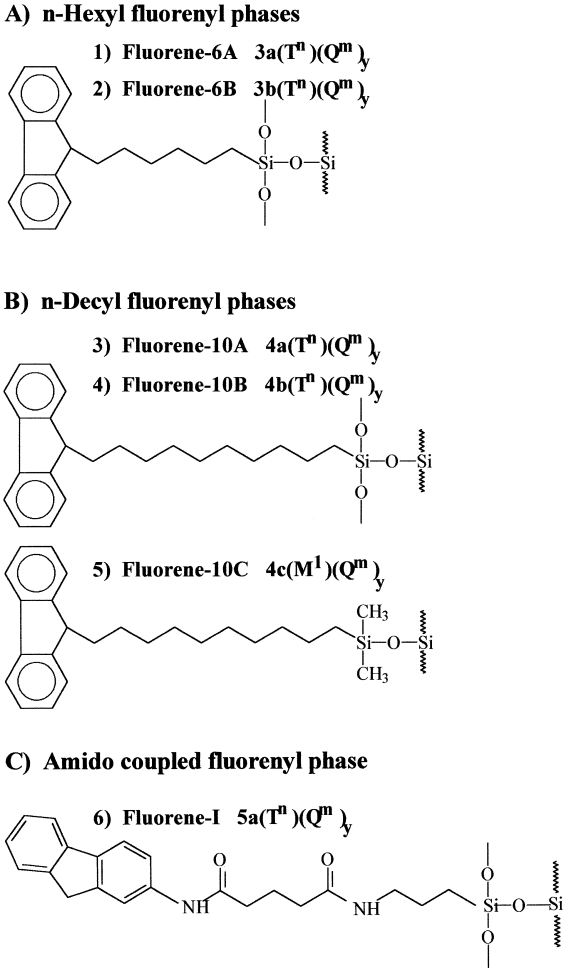

Fig. 1. Overview of the investigated fluorenyl phases. Each fluorenyl phase consists of silica gel with an average particle size of 5 μm and an average pore diameter of 200 Å. The organic ligand was immobilized on the silica gel surface either by employing trichlorosilane (fluorene-6A [$3a(T^n)(Q^m)_y$] No. 1, fluorene-10A [$4a(T^n)(Q^m)_y$] No. 3), monochlorosilane (fluorene-10C [$4c(M^1)(Q^m)_y$] No. 5), or triethoxysilane (fluorene-6B [$3b(T^n)(Q^m)_y$] No. 2, fluorene-10B [$4b(T^n)(Q^m)_y$] No. 4, fluorene-I [$5a(T^n)(Q^m)_y$] No. 6). Ligand densities of the attached fluorenyl fragments, No. 1: 3.98 μmol/m^2, No. 2: 1.24 μmol/m^2, No. 3: 3.69 μmol/m^2, No. 4: 0.9 μmol/m^2, No. 5: 1.77 μmol/m^2, No. 6: 1.62 μmol/m^2.

tive fragment decays during the impact of the inserted waiting period. This effect is increased by replacing the waiting period with a twelve-pulse sequence. The magnetization of the more mobile fragments with weaker dipolar-coupled protons is refocused, whereas the magnetization of the less mobile fragments with stronger dipolar-coupled protons is dephased by the impact of the twelve-pulse sequence. Therefore, statements about the mobility of fluorenyl phases, or differences in the mobility of the respective phase fragments can be made by varying the window (waiting period) between the pulses of the twelve-pulse sequence.

The effect of the dipolar filter on the ^{13}C-CP-MAS-NMR spectra of the fluorenyl phases fluorene-10A [$4a(T^n)(Q^m)_y$] and fluorene-10B [$4b(T^n)(Q^m)_y$] is illustrated in Figs. 2 and 3. In the case of the phase fluorene-10B [$4b(T^n)(Q^m)_y$], the unconverted ethoxy groups seem to have a higher mobility compared to the residual ligand fragments, because their signal is clearly detected even at a larger window of 15 μs. However, the signal intensities of the other ligand fragments seem to decrease at the same rate. But these stacked-plot graphics can just be used for providing a first impression about the mobility of the different ligand fragments of the respective stationary phase. For a more detailed judgement and comparison of the mobility of the investigated phases, the effect of the dipolar filter has to be studied more closely.

At this point it must be emphasized that each of the dipolar filter NMR spectra of the same fluorenyl phase has to be recorded with an analogous number of transients. But for each fluorenyl phase an individual number of transients was used to obtain a reasonable signal-to-noise ratio, depending on their ligand density. To minimize the influence of the number of applied transients and the differences in the quality of the adjusted Hartmann–Hahn condition, the dipolar filter spectra were analyzed as follows: First, the integral values of the fragment signals were determined. Then, these integral values were correlated for each fluorenyl phase by setting the integral value of the fragment signals to 100% for the spectrum recorded with the smallest window between the sequence pulses. Although, just signal intensities from fragments with the same cross polarization efficiency can be compared with each other in a single ^{13}C-CP-MAS-NMR spectrum, the effect of the different cross polarization efficiencies are averaged by this method. Therefore, the procedural decline of the integral intensity from aromatic fragments can be compared with those from

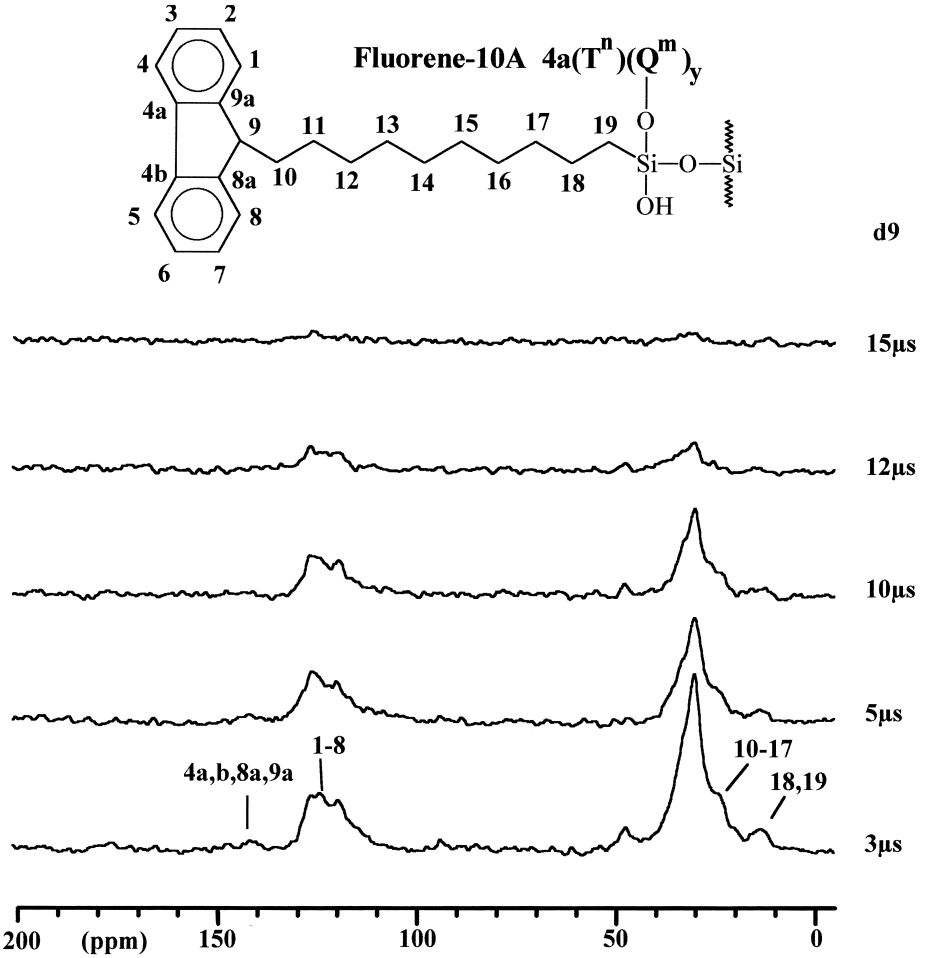

Fig. 2. Impact of the dipolar filter on the ^{13}C-CP-MAS-NMR spectra of the stationary phase fluorene-10A [4a(T^n)(Q^m)$_y$] (rotation frequency: 4 kHz). Information about the fragment mobility is provided by the variation of the window (waiting time d9) between the pulses of the twelve-pulse sequence.

aliphatic fragments. Figs. 4 and 5 exhibit the procedural decline of those fragment signals for each fluorenyl phase, depending on the impact of the dipolar filter. Some interesting trends are recognizable by a close observation of the depicted data.

The biggest fluctuations in these curves are observed for the fluorenyl phases with a lower ligand density, because the worse signal-to-noise ratio is responsible for a greater inaccuracy in measurement compared to fluorenyl phases with a higher ligand density. In most cases the integral values of the aromatic fragments are a little bit larger than those of the aliphatic fragments for the individual stationary phase. But these values decline approximately with the same rate, indicating a comparable mobility for the individual fragments of the same stationary phase. The fastest dephasing was recorded for the magnetization of the amido coupled phase fluorene-I [5a(T^n)(Q^m)$_y$], indicating the lowest system mobility of all investigated phases. In the case of the *n*-alkyl fluorenyl phases a small increase of the system mobility is found for the phases with a lower ligand density. Despite the above mentioned measuring inaccuracy, which is usually around 2% and can grow up to 5% for very badly resolved spectra, this tendency is beyond doubt, because at larger windows

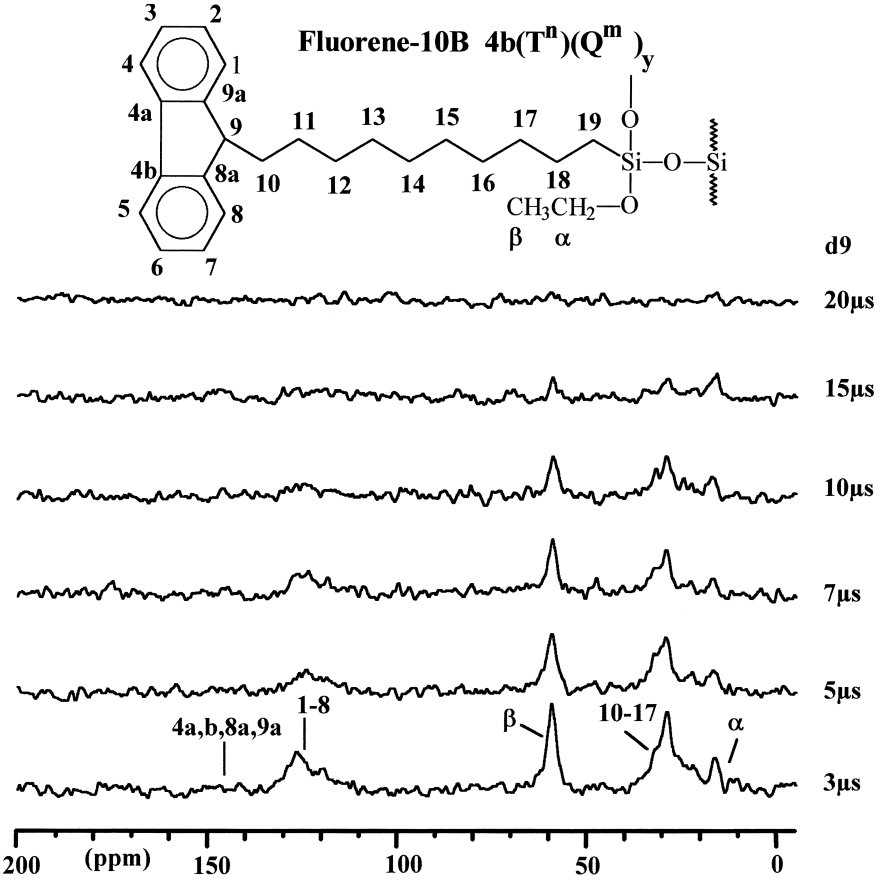

Fig. 3. Impact of the dipolar filter on the ^{13}C-CP-MAS-NMR spectra of the stationary phase fluorene-10B [4c(M^1)(Q^m)$_y$] (rotation frequency: 4 kHz).

a small percentage of the respective signals is clearly detected for the phases with a low ligand density, whereas the magnetization of the other phases is totally dephased already.

The effect of the dipolar filter can also be investigated by ^{1}H-NMR detection. In contrast to ^{13}C-NMR detection, no spin diffusion has to be considered, which might play a role during the cross polarization time, especially in the case of rather rigid systems. Unfortunately, strong homonuclear dipolar interactions of the protons are a limiting factor for the resolution of solid-state NMR spectra with ^{1}H detection. Therefore, much higher rotation frequencies (14 kHz) had to be applied for ^{1}H dipolar filter NMR measurements. An additional problem exists at this high rotation frequency, because windows larger than 50 µs are in the range of a single rotor revolution. For each of the investigated fluorenyl phases, intensity fluctuations due to artefacts or phasing errors were observed at windows of that size. Therefore, just windows up to 30 µs are considered in the following section.

The impact of the dipolar filter by ^{1}H detection on the phases fluorene-6B [3b(T^n)(Q^m)$_y$], and fluorene-10A [4a(T^n)(Q^m)$_y$] is illustrated in Figs. 6 and 7. Analogous to the ^{13}C detection, the procedural decline of the aromatic and aliphatic fragment signals, depending on the impact of the dipolar filter, is shown in Figs. 8 and 9 for the two above mentioned phases as well as for fluorene-I [5a(T^n)(Q^m)$_y$]. The integral values of the those fragment signals were determined by peak deconvolution

In contrast to the experiments with ^{13}C detection, more significant differences in the fragment mobility

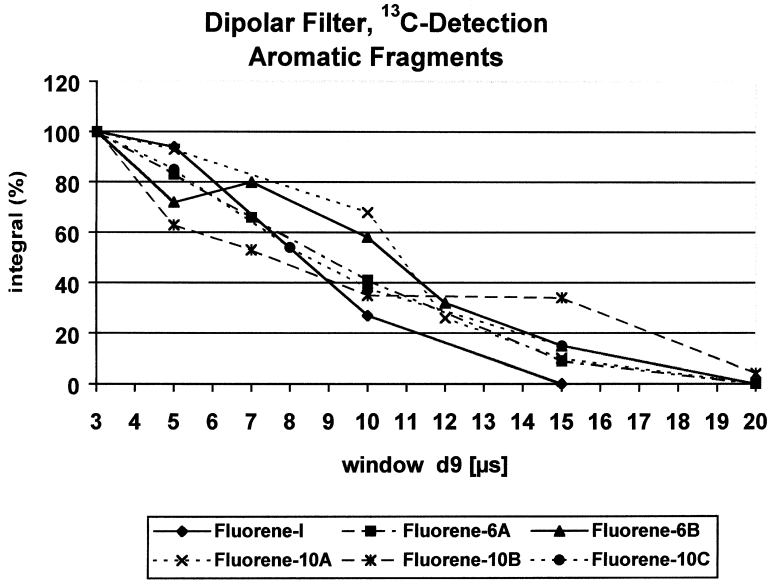

Fig. 4. Impact of the dipolar filter on the aromatic ligand fragments of the ^{13}C-CP-MAS-NMR spectra of the investigated fluorenyl phases fluorene-6A [3a(T^n)(Q^m)$_y$], fluorene-6B [3b(T^n)(Q^m)$_y$], fluorene-10A [4a(T^n)(Q^m)$_y$], fluorene-10B [4b(T^n)(Q^m)$_y$], fluorene-10C [4c(M^1)(Q^m)$_y$], and fluorene-I [5a(T^n)(Q^m)$_y$] (rotation frequency: 4 kHz).

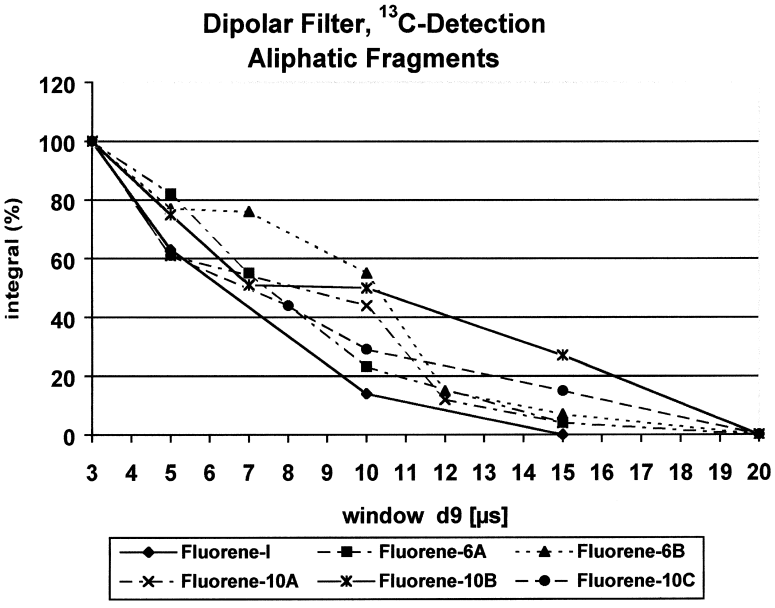

Fig. 5. Impact of the dipolar filter on the aliphatic ligand fragments of the ^{13}C-CP-MAS-NMR spectra of the investigated fluorenyl phases fluorene-6A [3a(T^n)(Q^m)$_y$], fluorene-6B [3b(T^n)(Q^m)$_y$], fluorene-10A [4a(T^n)(Q^m)$_y$], fluorene-10B [4b(T^n)(Q^m)$_y$], fluorene-10C [4c(M^1)(Q^m)$_y$], and fluorene-I [5a(T^n)(Q^m)$_y$] (rotation frequency: 4 kHz).

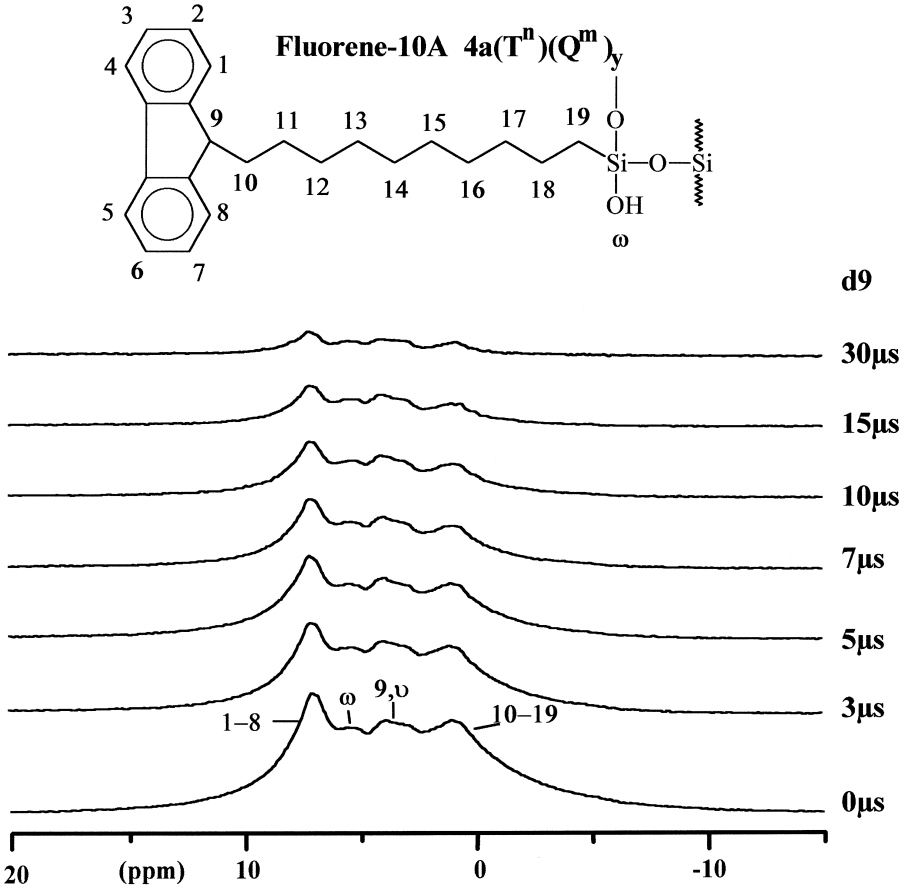

Fig. 6. Impact of the dipolar filter on the ^{1}H-MAS-NMR spectra of the stationary phase fluorene-10A [4a(T^n)(Q^m)$_y$] (rotation frequency: 14 kHz).

of the same fluorenyl phase can be observed by ^{1}H detection. In the case of the phases fluorene-6A [3a(T^n)(Q^m)$_y$] and fluorene-10A [4a(T^n)(Q^m)$_y$], the aromatic ligand fragments are a little bit more mobile, whereas they are much less mobile than the aliphatic fragments in the case of the phases fluorene-6B [3b(T^n)(Q^m)$_y$] and fluorene-I [5a(T^n)(Q^m)$_y$]. But for the latter phases the signal of the aliphatic ligand fragments is superimposed with the signal of the unconverted ethoxy groups, which possess a higher mobility. Due to this superposition, the mobility of the aliphatic fragments cannot be compared between the individual fluorenyl phases (Fig. 8). However, the aromatic ligand fragments can be compared with respect to their mobility. In Fig. 9 the same tendency is found for the investigated fluorenyl phases as for the respective spectra with ^{13}C detection. The aromatic ligand fragments of the amido coupled phase fluorene-I [5a(T^n)(Q^m)$_y$] are less mobile compared to *n*-alkyl fluorenyl phases. The lower the ligand density of the *n*-alkyl fluorenyl phases, the higher is the mobility of their aromatic ligand fragments.

In comparison to the analogous experiments by ^{13}C detection, the big advantage of the approach by ^{1}H detection is an immense saving of time for the acquisition of a single spectrum, due to the natural abundance of the detected nuclei. Especially for phases with a low ligand density this time factor by far compensates the disadvantage of the smaller chemical shift dispersion and the worsening resolution due to stronger dipolar interactions.

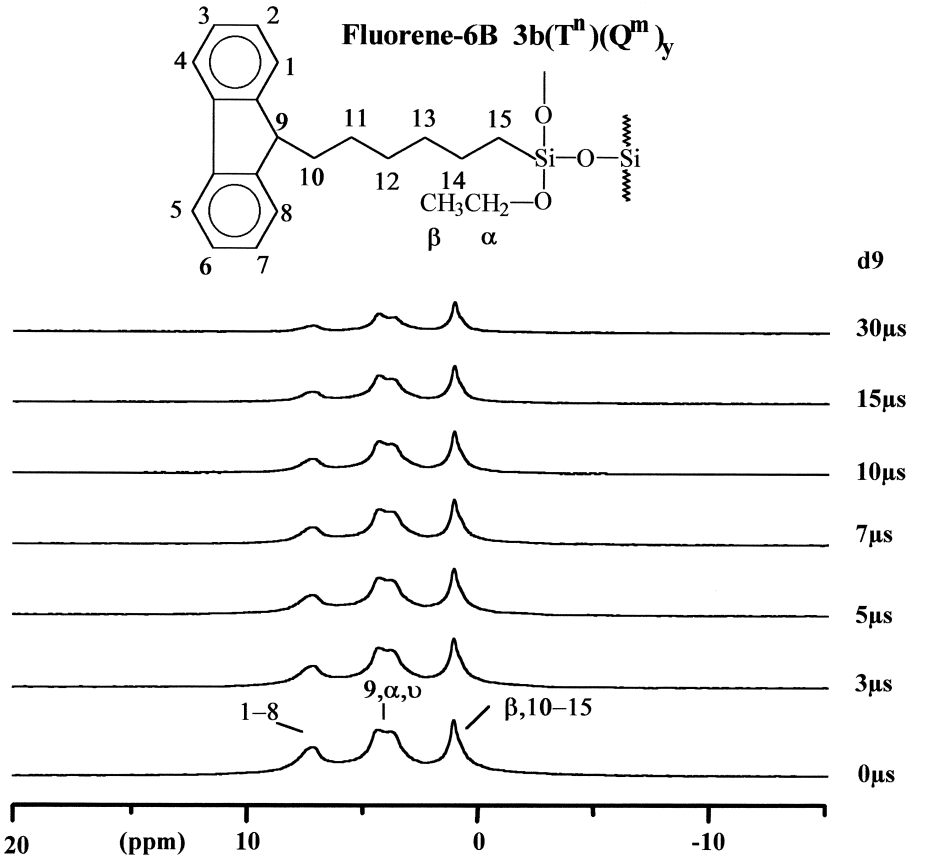

Fig. 7. Impact of the dipolar filter on the ^{1}H-MAS-NMR spectra of the stationary phase fluorene-6B [3b(T^{n})(Q^{m})$_{y}$] (rotation frequency: 14 kHz).

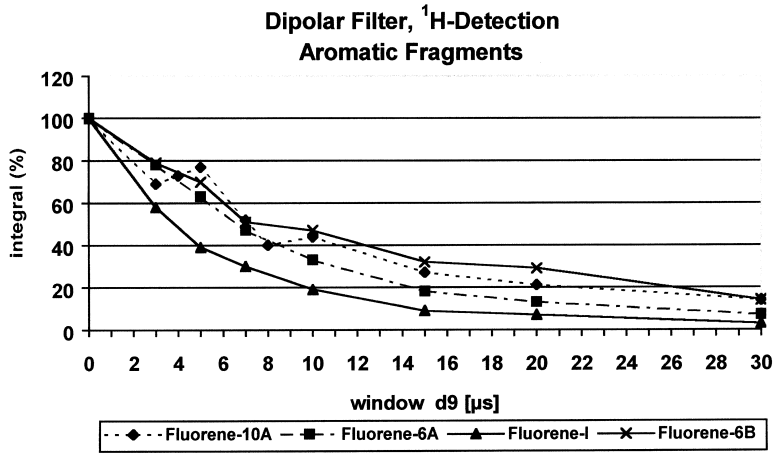

Fig. 8. Impact of the dipolar filter on the aromatic ligand fragments of the ^{1}H-MAS-NMR spectra of the investigated fluorenyl phases fluorene-6A [3a(T^{n})(Q^{m})$_{y}$], fluorene-6B [3b(T^{n})(Q^{m})$_{y}$], fluorene-10A [4a(T^{n})(Q^{m})$_{y}$], and fluorene-I [5a(T^{n})(Q^{m})$_{y}$] (rotation frequency: 14 kHz).

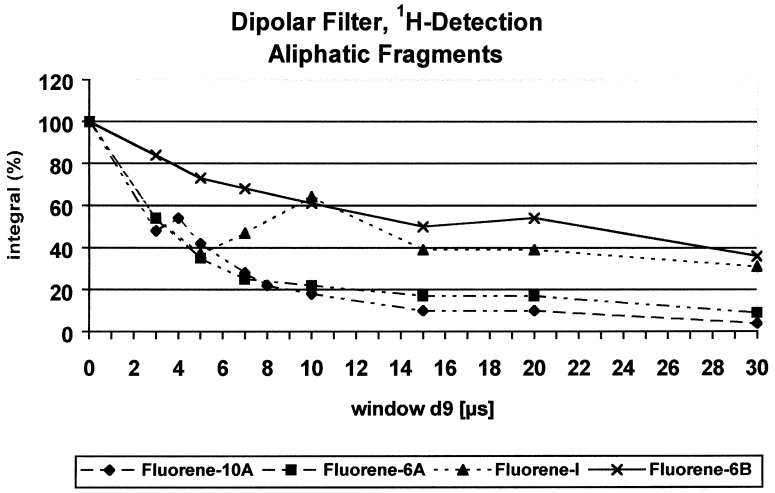

Fig. 9. Impact of the dipolar filter on the aliphatic ligand fragments of the ^{1}H-MAS-NMR spectra of the investigated fluorenyl phases fluorene-6A [3a(T^n)(Q^m)$_y$], fluorene-6B [3b(T^n)(Q^m)$_y$], fluorene-10A [4a(T^n)(Q^m)$_y$], and fluorene-I [5a(T^n)(Q^m)$_y$] (rotation frequency: 14 kHz).

3.1.2. Variation of the contact time

The cross polarization constant T_{CH} is sensitive to motions in the lower kHz region. It is available by the contact time variation experiment, where the signal intensity is a function of the contact time. The size of T_{CH} depends on both, the mobility of the respective fragment and the number of neighboring protons. If this number is similar or equal for different carbon atoms then the size of T_{CH} is comparable. The higher the mobility of the respective fragment, the greater is the size of its T_{CH} value [32,45].

The T_{CH} values of the investigated *n*-alkyl fluorenyl phases are presented in Table 1. The same trend is observed for either the aromatic and the aliphatic ligand fragments. The lower the ligand density of the respective *n*-alkyl fluorenyl phase, the higher is their mobility. Just the T_{CH} values of fluorene-10B [4b(T^n)(Q^m)$_y$] (aromatic fragments) and fluorene-6B [3b(T^n)(Q^m)$_y$] (aliphatic fragments) do not fit into this trend. In both cases the signal-to-noise ratio was rather bad due to the low ligand density. Therefore, this exception can probably be explained by the low intensity of the respective

Table 1
Cross polarization constants T_{CH} (µs) of the *n*-alkyl fluorenyl phases fluorene-6A [3a(T^n)(Q^m)$_y$], fluorene-6B [3b(T^n)(Q^m)$_y$], fluorene-10A [4a(T^n)(Q^m)$_y$], fluorene-10B [4b(T^n)(Q^m)$_y$], and fluorene-10C [4c(M^1)(Q^m)$_y$] with respect to their ligand density α [µmol/m^2]. Each spectra was detected by ^{13}C-CP-MAS NMR spectroscopy at a rotation frequency of 4 kHz. Assignment of the respective carbon atoms according to Figs. 2 and 3

	T_{CH} values of *n*-alkyl fluorenyl phases				
Phase/carbon atoms	1–3,6–8	12–16	α	β	
Fluorene-10B [4b(T^n)(Q^m)$_y$] (α=0.9)	56	84	97	378	
Phase/carbon atoms	1–3,6–8	12,13	α	β	11,14
Fluorene-6B [3b(T^n)(Q^m)$_y$] (α=1.24)	77	20	65	208	41
Phase/carbon atoms	1–3,6–8	12–16	4a,b,8a,9a		
Fluorene-10C [4c(M^1)(Q^m)$_y$] (α=1.77)	72	63	506		
Phase/carbon atoms	1–3,6–8	12–16	4a,b,8a,9a	18,19	
Fluorene-10A [4a(T^n)(Q^m)$_y$] (α=3.69)	69	58	807	65	
Phase/carbon atoms	1–3,6–8	10,12–14	4a,b,8a,9a	11	15
Fluorene-6A [3a(T^n)(Q^m)$_y$] (α=3.98)	61	48	663	46	54

fragment because it causes a much higher measuring inaccuracy for the respective T_{CH} value compared to other, much better resolved fragment signals. The large T_{CH} values of the unconverted ethoxy groups from fluorene-6B [3b(T^n)(Q^m)$_y$] and fluorene-10B [4b(T^n)(Q^m)$_y$] are another interesting finding. Analogous to the results of the dipolar filter experiments (Fig. 3), the unconverted ethoxy groups seem to have a much higher mobility than the residual ligand fragments.

3.1.3. $T_{1\rho H}$ measurements

The spin-lattice relaxation times in the rotating frame ($T_{1\rho H}$) by ^{13}C detection are a further parameter of ligand mobility. $T_{1\rho H}$ values, which are characteristic for motions in the mid-kHz region, were received by the method of Schaefer and Stejskal [46,47]. The dependance of relaxation times on temperature is called the correlation time curve. Relaxation times, which are declining with decreasing temperature, correspond to a higher mobility of the investigated carbon atoms and this is characteristic for the left branch of the correlation time curve. On the other hand $T_{1\rho H}$ values, located on the right branch of the correlation time curve, are declining with increasing temperature which means a lower mobility of the carbon atoms [31,46,47].

The $T_{1\rho H}$ values of the phases fluorene-6A [3a(T^n)(Q^m)$_y$] and fluorene-10A [4a(T^n)(Q^m)$_y$] are shown at Table 2. In both cases the lowest $T_{1\rho H}$ values are observed for the measurements at 310 K. Systems with $T_{1\rho H}$ values shifting around the curve's minimum correspond to a medium mobility.

The determination of $T_{1\rho H}$ values by direct ^1H detection without cross polarization is a further alternative which provides information about the system mobility. Analogous to the dipolar filter technique an immense saving of time is the big advantage for the determination of $T_{1\rho H}$ values with this method. Table 3 depicts the $T_{1\rho H}$ values of the aromatic and aliphatic ligand fragments for the five *n*-alkyl fluorenyl phases and the amido coupled fluorenyl phase. In the case of the *n*-alkyl fluorenyl phases the $T_{1\rho H}$ values of the aromatic protons are located clearly on the left branch of the correlation time curve, whereas the $T_{1\rho H}$ values of fluorene-I [5a(T^n)(Q^m)$_y$] shift around the curve's minimum. The lower the ligand density the larger are the $T_{1\rho H}$ values of the *n*-alkyl fluorenyl phases, indicating a higher mobility of the respective aromatic ligand fragment. The same trend is observed for the aliphatic ligand fragments, but in accordance to the dipolar filter measurements the superposition of the signal from the aliphatic protons with the signal of the unconverted ethoxy protons has to be noticed. Due to the high amount of unconverted ethoxy groups these $T_{1\rho H}$ values of fluorene-10B [4b(T^n)(Q^m)$_y$] and fluorene-6B [3b(T^n)(Q^m)$_y$] are much larger compared to the other fluorenyl phases. Therefore, these two $T_{1\rho H}$ values represent mainly the mobility of the unconverted ethoxy groups instead of the alkyl chain fragments. The $T_{1\rho H}$ values of fluorene-I [5a(T^n)(Q^m)$_y$] are much smaller, because this phase is very well cross linked and has a rather small amount of unconverted ethoxy groups.

The $T_{1\rho H}$ values emphasize the observation from the other dynamic methods about an increased

Table 2
Temperature dependence of the $T_{1\rho H}$ values (ms) of the two phases fluorene-6A [3a(T^n)(Q^m)$_y$] and fluorene-10A [4a(T^n)(Q^m)$_y$] detected by ^{13}C-CP-MAS NMR spectroscopy at a rotation frequency of 4 kHz. Assignment of the respective carbon atoms according to Figs. 2 and 3

	$T_{1\rho H}$ values of the phase Fluorene-6A [3a(T^n)(Q^m)$_y$]				
Temp./carbon atoms	4a,b,8a,9a	1–3,6–8	10,12–14	11	15
295 K	3.11	3.15	2.89	2.76	3.61
310 K	2.33	2.24	2.22	2.32	1.91
325 K	2.72	2.83	2.49	2.52	2.33
	$T_{1\rho H}$ values of the phase Fluorene-10A [4a(T^n)(Q^m)$_y$]				
Temp./carbon atoms	4a,b,8a,9a	1–3,6–8	12–16	18,19	
295 K	2.04	2.59	2.40	2.42	
310 K	1.92	1.41	1.53	2.09	
325 K	2.94	2.37	2.38	3.07	

Table 3
Temperature dependence of the $T_{1\rho H}$ values (ms) for all investigated fluorenyl phases fluorene-6A [3a(T^n)(Q^m)$_y$], fluorene-6B [3b(T^n)(Q^m)$_y$], fluorene-10A [4a(T^n)(Q^m)$_y$], fluorene-10B [4b(T^n)(Q^m)$_y$], fluorene-10C [4c(M^1)(Q^m)$_y$], and fluorene-I [5a(T^n)(Q^m)$_y$] with respect to their ligand density α (μmol/m^2). Each spectra was detected by ^{1}H-MAS-NMR spectroscopy at a rotation frequency of 14 kHz. Assignment of the respective protons according to Figs. 6 and 7

	$T_{1\rho H}$ values of Fluorene-10B [4b(T^n)(Q^m)$_y$] (α=0.9)			
Proton/temp.	295 K	305 K	315 K	325 K
1–8	8.30	9.08	10.44	11.83
β, 12–18	19.49	22.17	24.24	26.64
	$T_{1\rho H}$ values of Fluorene-6B [3b(T^n)(Q^m)$_y$] (α=1.24)			
Proton/temp.	295 K	305 K	315 K	325 K
1–8	7.36	8.91	10.55	12.49
β, 10–15	10.61	11.85	12.60	13.78
	$T_{1\rho H}$ values of Fluorene-10C [4c(M^1)(Q^m)$_y$] (α=1.77)			
Proton/temp.	295 K	305 K	315 K	325 K
1–8	4.62	5.39	6.05	7.37
10–19	2.46	2.81	3.23	3.87
	$T_{1\rho H}$ values of Fluorene-10A [4a(T^n)(Q^m)$_y$] (α=3.69)			
Proton/temp.	295 K	305 K	315 K	325 K
1–8	3.26	3.71	4.62	5.87
10–19	1.53	1.66	2.11	2.60
	$T_{1\rho H}$ values of Fluorene-6A [3a(T^n)(Q^m)$_y$] (α=3.98)			
Proton/temp.	295 K	305 K	315 K	325 K
1–8	3.69	4.11	4.80	5.79
10–15	1.05	1.28	1.65	1.93
	$T_{1\rho H}$ values of Fluorene-I [5a(T^n)(Q^m)$_y$] (α=1.62)			
Proton/temp.	295 K	305 K	315 K	325 K
1–8	3.85	4.47	4.20	4.40
β	2.93	2.67	2.89	2.94

mobility of *n*-alkyl fluorenyl phases as compared to the amido coupled fluorenyl phase. The $T_{1\rho H}$ NMR experiments demonstrated also an increasing system mobility by a decreasing ligand density for *n*-alkyl fluorenyl phases. The dependance of $T_{1\rho H}$ values on the applied radiation and rotation frequencies explain the observed differences in their localization on the correlation time curve for ^{13}C and ^{1}H detection.

3.2. HPLC Applications

3.2.1. PAHs

In the first part of this paper [25] the utility of the *n*-alkyl fluorenyl phases for HPLC separations of PAHs was demonstrated by using the Sander and Wise test (SRM 869) [28,29]. The selectivity of the *n*-alkyl fluorenyl phases for a second, more complex PAH test (SRM 1647/Fig. 10) is depicted in Fig. 11. Those 16 PAHs are regarded as priority pollutants according to the US Environmental Protection Agency (EPA, method 610) and are widely accepted as a demanding test to evaluate the chromatographic capability of stationary phases. Analogous to the Sander and Wise test, the *n*-alkyl fluorenyl phases showed a different separation behavior compared to *n*-alkyl phases. Whereas in the latter case a gradient elution program containing acetonitrile and water was used for a successful separation of the PAHs [3,48,49], the polarity of the mobile phase had to be raised by replacing acetonitrile with methanol in the case of *n*-alkyl fluorenyl phases.

A much better selectivity for the smaller PAHs 1–6 on the one hand as well as a decreasing selectivity and much longer retention times for the larger PAH molecules at a higher water content of the mobile phase on the other hand required the implementation of individual gradients for the phases fluorene-10A [4a(T^n)(Q^m)$_y$], fluorene-6A [3a(T^n)(Q^m)$_y$] and fluorene-10C [4c(M^1)(Q^m)$_y$]. The best selectivity of all investigated fluorenyl phases was obtained with the phase fluorene-10A [4a(T^n)(Q^m)$_y$]. As shown in Fig. 11a, 15 out of 16 PAHs could be separated on this phase; just the PAH set 9/10 remained unresolved. Set 11/12 was a further unresolved PAH set on the phases fluorene-6A [3a(T^n)(Q^m)$_y$] and fluorene-10C [4c(M^1)(Q^m)$_y$] (Fig. 11b and c). The two *n*-alkyl fluorenyl phases fluorene-6B [3b(T^n)(Q^m)$_y$] and fluorene-10B [4b(T^n)(Q^m)$_y$] with a lower ligand density did not possess any satisfactory selectivity for the PAH sample SRM 1647. Their separation behavior tested under various mobile phase compositions is characterized by badly resolved or coeluting PAH sets, as illustrated in Fig. 11d for the phase fluorene-10B [4b(T^n)(Q^m)$_y$].

3.2.2. Nitro explosives

Besides the PAHs the separation of nitro explosives is regarded as another important task in environmental analysis. Therefore, the *n*-alkyl fluorenyl phases have had their separation behavior examined

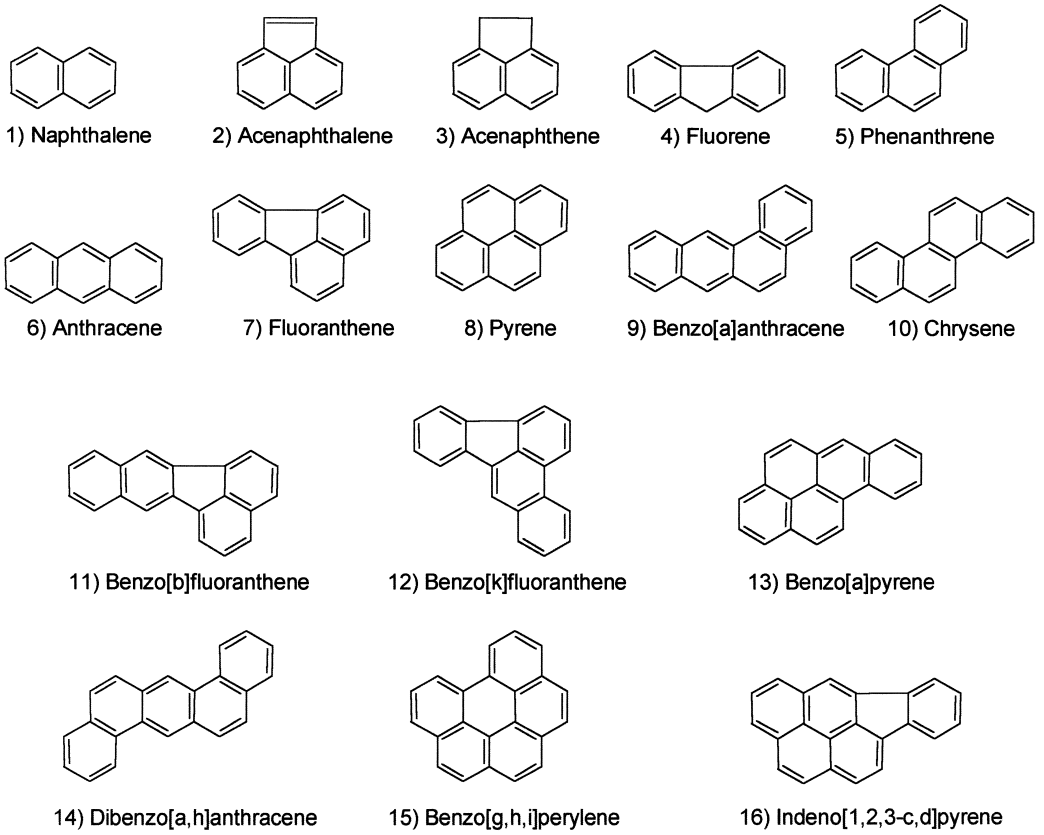

Fig. 10. Structures of 16 PAHs (test SRM 1647) regarded as priority pollutants.

for nitro explosives, because it is of high interest working with the same kind of stationary phases on different areas of applications. The employed test mixture, containing two heterocyclic as well as two aromatic molecules each, with one, two, or three attached nitro groups, respectively, is depicted in Fig. 12. The best selectivity was obtained on the phase fluorene-6A [3a(T^n)(Q^m)$_y$] (Fig. 13a) using a mobile phase composition of methanol–water (50:50, v/v). The first detected peak belongs to the two heterocyclic solute molecules, followed by the peaks of aromatic nitro explosives. The latter were eluted a significant order from the trifunctional phase fluorene-6A [3a(T^n)(Q^m)$_y$] with a *n*-hexyl spacer. Solute molecules with a single nitro group are eluted first, followed by the molecules with two and, finally, three nitro substituents. In contrast to this elution order, a totally different separation behavior for the aromatic nitro explosives was detected using the monofunctional phase fluorene-10C [4c(M^1)(Q^m)$_y$] with a *n*-decyl spacer (Fig. 13b). In this case, the best separation was obtained by a methanol–water ratio of 40:60 instead of 50:50. Here, the trinitro compounds 7 and 8 are eluted prior to the di- and mononitro compounds 3–6. From this group the mononitro compound 4 is retarded the strongest and the three other molecules cannot be separated using fluorene-10C [4c(M^1)(Q^m)$_y$] as stationary phase. Unfortunately, just peak broadening instead of a better selectivity was obtained by a further increase of the polarity of the mobile phase.

A combination of the two contrary elution orders described above was found for the phase fluorene-10A [4a(T^n)(Q^m)$_y$]. At a methanol–water ratio of 50:50, no clear elution order was recognizable by a rather bad selectivity for the aromatic solutes. The trinitro solute 7 eluted first, followed by a coelution of 3, 6, and 8, or 4 and 5, respectively. An increase

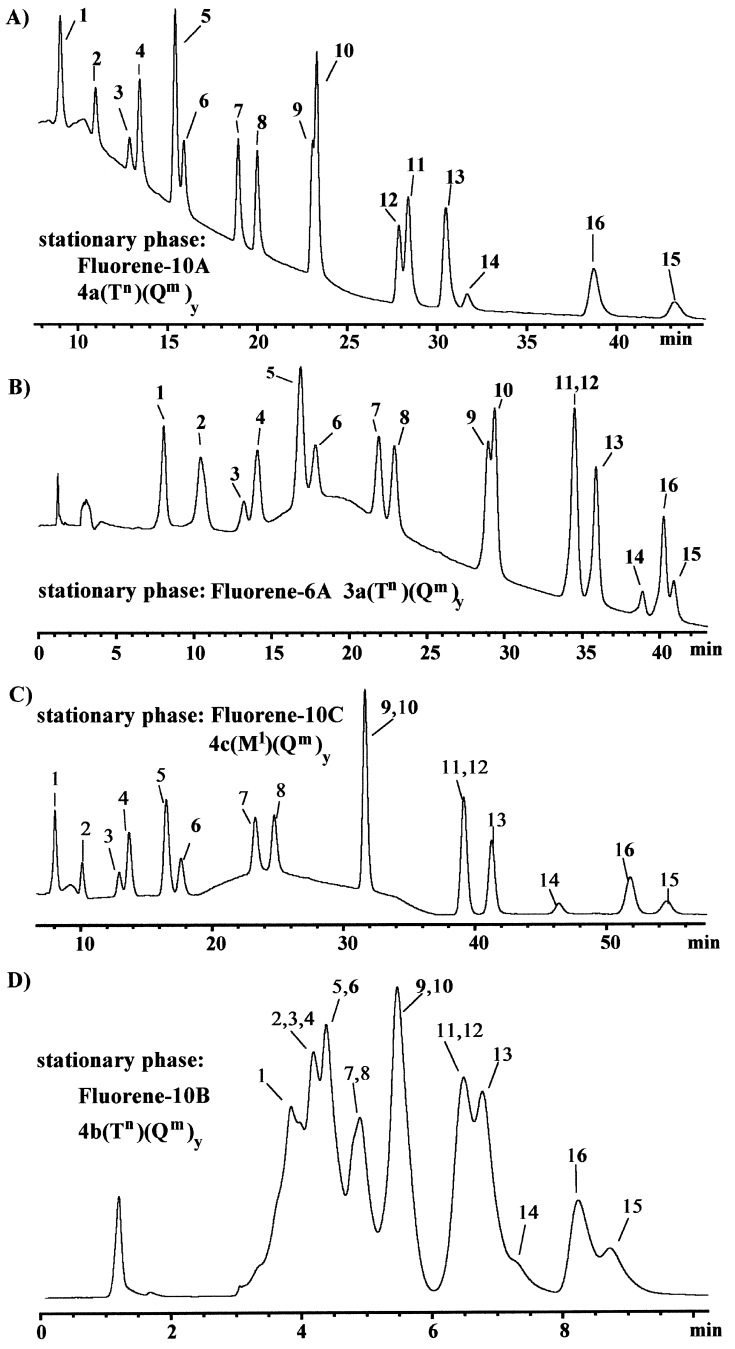

Fig. 11. Separation of the PAH test SRM 1647 shown in Fig. 10. Conditions in all cases were as follows: Temperature, 25°C; wavelength, 254 nm; flow-rate: 1 ml/min. (A) Stationary phase, fluorene-10A [4a(T^n)(Q^m)$_y$]; mobile phase; a 20 min linear gradient from methanol–water (70:30, v/v) to (90:10, v/v), and hold until the end of the separation. (B) Stationary phase, fluorene-6A [3a(T^n)(Q^m)$_y$]; mobile phase, a 10 min hold at methanol–water (70:30, v/v), a 30 min linear gradient to methanol–water (90:10, v/v), and hold until the end of the separation. (C) Stationary phase, fluorene-10C [4c(M^1)(Q^m)$_y$]; mobile phase, a 15 min hold at methanol–water (70:30, v/v), a 15 min linear gradient to methanol–water (80:20, v/v), and hold until the end of the separation. (D) Stationary phase, fluorene-10B [4b(T^n)(Q^m)$_y$]; mobile phase, isocratic separation with methanol–water (80:20, v/v).

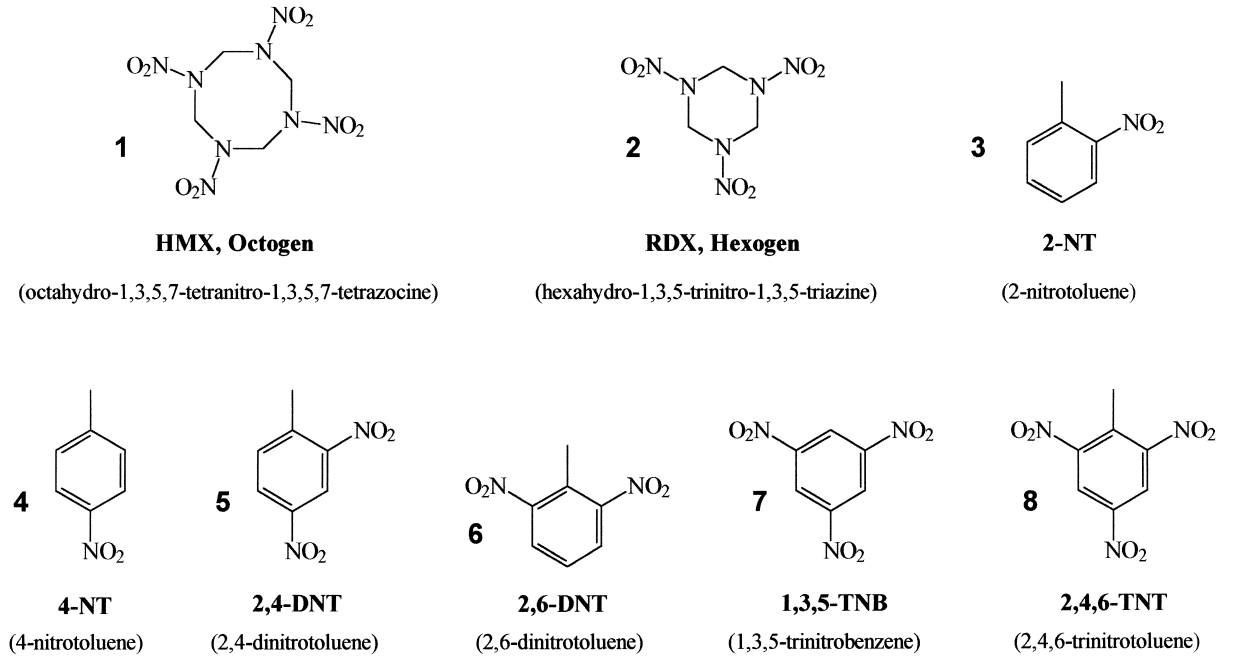

Fig. 12. Structures of the nitro explosives.

of the water content of the mobile phase to 60% resulted in a better selectivity (Fig. 13c), the elution order becomes more similar to the one attained for the phase fluorene-10C [4c(M^1)(Q^m)$_y$]. But the dinitro compound 5 is still more strongly retarded than the mononitro compound 3, also indicating similarities to the elution order of the phase fluorene-6A [3a(T^n)(Q^m)$_y$.

In Fig. 13d the selectivity of the phase fluorene-6B [3b(T^n)(Q^m)$_y$] is also depicted. Due to the low ligand density, the selectivity for the investigated sample of nitro explosives is not satisfactory. The same problem was observed for the PAHs as mentioned in the previous chapter. More interesting is a second feature of this phase. Despite this unsatisfactory selectivity the same elution order of the solute molecules can be detected as for the phase fluorene-6A [3a(T^n)(Q^m)$_y$] with a high ligand density.

4. Discussion

n-Alkyl fluorenyl phases were developed in order to obtain stationary phases with a higher system mobility compared to amido coupled fluorenyl phases. An improved mobility of *n*-alkyl fluorenyl phases was already indicated by conventional ^{1}H-MAS-NMR spectroscopy in the first part of this paper. The results obtained from the more precise solid-state NMR dynamic measurement techniques confirm the higher mobility of *n*-alkyl fluorenyl phases compared to amido coupled fluorenyl phases. Furthermore, differences in the system mobility of the individual *n*-alkyl fluorenyl phases were also observed by these measurements. The chain length of the *n*-alkyl spacer did not have a considerable influence on the system mobility of the investigated *n*-alkyl fluorenyl phases. The ligand density is the deciding factor for the mobility of the whole ligand system. The same trends were observed by each of the applied techniques. The lower the ligand density the higher is the system mobility of the *n*-alkyl fluorenyl phases. The system mobility of the amido coupled fluorenyl phase was the lowest one of all the investigated fluorenyl phases.

Parameters like the signal-to-noise ratio (^{13}C detection), the superposition of fragment signals, or the worsening resolution due to strong dipolar inter-

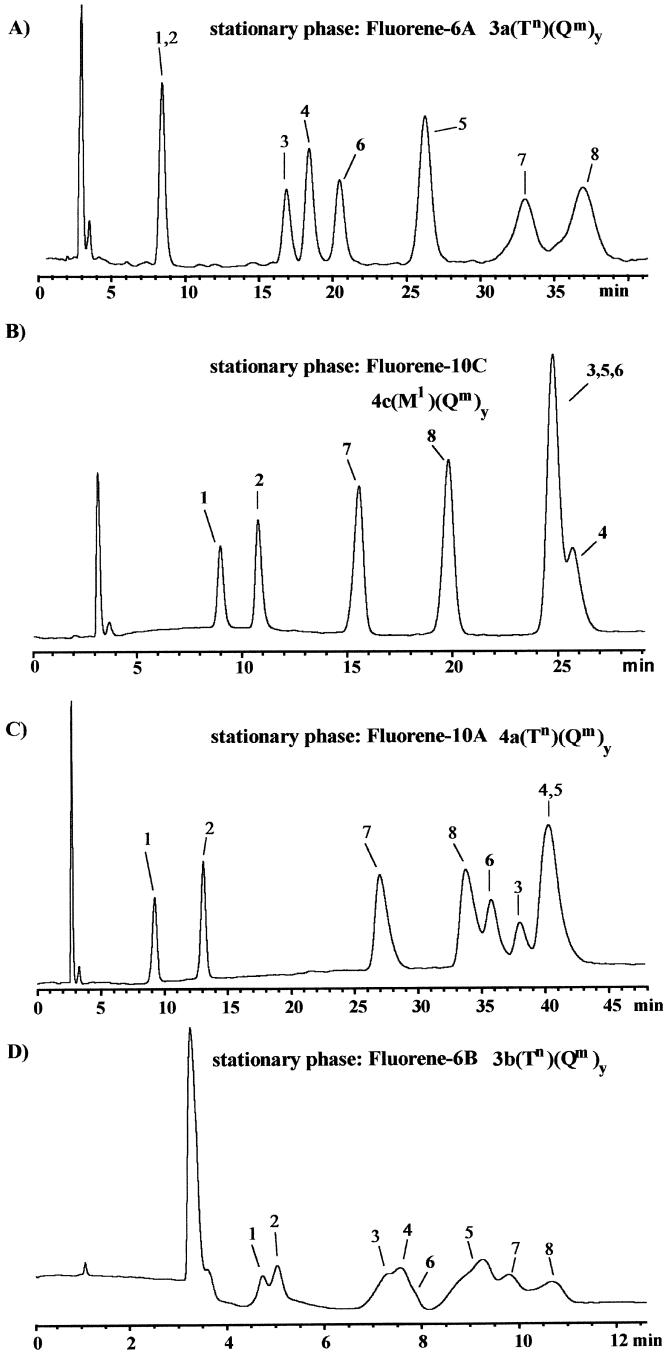

Fig. 13. Separation of nitro explosives shown in Fig. 12. Conditions in all cases were as follows: Temperature, 25°C; wavelength, 254 nm; flow-rate: 1 ml/min. (A) Stationary phase, fluorene-6A [3a(T^n)(Q^m)$_y$]; mobile phase, methanol–water (50:50, v/v); (B) Stationary phase, fluorene-10C [4c(M^1)(Q^m)$_y$]; mobile phase, methanol–water (40:60, v/v); (C) Stationary phase, fluorene-10A [4a(T^n)(Q^m)$_y$]; mobile phase, methanol–water (40:60, v/v); (D) Stationary phase, fluorene-6B [3b(T^n)(Q^m)$_y$]; mobile phase, methanol–water (50:50, v/v).

actions (^{1}H detection) are limiting factors for comparing the dynamic behavior of the investigated phases by just a single dynamic measurements technique. Therefore, the results of all different techniques have to be regarded and correlated with each other for a correct classification of the system mobility.

It was shown that the dipolar filter technique is a very graphic method for obtaining information about the system mobility. A small increase of the mobility of the aromatic ligand fragments compared to the aliphatic fragments was detected for most of the *n*-alkyl fluorenyl phases. The results of the $T_{1\rho H}$ measurements by ^{1}H detection confirm this observation. In each case the $T_{1\rho H}$ values of the aromatic protons are a little bit larger than the $T_{1\rho H}$ values of the aliphatic protons. The only exception are the phases fluorene-6B [3b(T^n)(Q^m)$_y$] and fluorene-10B [4b(T^n)(Q^m)$_y$] due to the superposition of the signals from the aliphatic and the unconverted ethoxy protons. But similarities in the declining rate of the integral values on the impact of the dipolar filter and in the size of the $T_{1\rho H}$ values are an indication for a comparable mobility of the different ligand fragments of an individual fluorenyl phases. The $T_{1\rho H}$ values are located on the left branch of the correlation time curve close to the curve's minimum. This corresponds to a medium mobility of the *n*-alkyl fluorenyl phases. Therefore, the mobility of these phase is in between the mobility of *n*-alkyl phases and amido coupled aromatic phases. For *n*-alkyl phases much higher $T_{1\rho H}$ values were reported [4], located clearly on the left branch of the correlation time curve, whereas the $T_{1\rho H}$ values of fluorene-I [5a(T^n)(Q^m)$_y$] and other amido coupled aromatic phases shift around the curve's minimum [19,20,27]. This means that these phases have a small to medium mobility. But especially the $T_{1\rho H}$ values of *n*-alkyl fluorenyl phases with a high ligand density are not much larger than the $T_{1\rho H}$ values of the amido coupled phase fluorene-I [5a(T^n)(Q^m)$_y$]. In accordance with the results of the dipolar filter experiments, *n*-alkyl fluorenyl phases with a high ligand density are regarded as just a little bit more mobile than the amido coupled phase fluorene-I [5a(T^n)(Q^m)$_y$].

By different solid-state NMR dynamic measurement techniques it was demonstrated that the length of the alkyl spacer has no considerable influence on the system mobility of the *n*-alkyl fluorenyl phases, whereas it plays a significant role during the separation process.

The important contribution of $\pi-\pi$ interactions due to significant interaction of aromatic ligand fragments in the separation process was already discussed in the first part of this paper. Compared to conventional polymeric C_{18} phases, *n*-alkyl fluorenyl phases have a different separation behavior for the PAH sample molecules of the Sander and Wise test. Differences in the length of the *n*-alkyl spacer caused differences in the elution order. The two phases with a *n*-hexyl spacer showed the largest differences in respect to polymeric C_{18} phases. It was also shown that retention times depend strongly on the amount of chemically bonded fluorene. A sufficient amount of attached *n*-alkyl fluorenyl fragments acting as the main interaction centers is required for obtaining a good selectivity during the separation process.

These trends were confirmed by the application of more demanding test samples. The application of the more complex PAH sample SRM 1647 demonstrated clearly that only phases synthesized with chorosilanes (fluorene-6A [3a(T^n)(Q^m)$_y$], fluorene-10A [4a(T^n)(Q^m)$_y$], and fluorene-10C [4c(M^1)(Q^m)$_y$]) are appropriate for PAH separations. Due to their higher ligand density in contrast to phases synthesized with ethoxysilanes (fluorene-6B [3b(T^n)(Q^m)$_y$] and fluorene-10B [4b(T^n)(Q^m)$_y$]), these phases contain a sufficient amount of interaction centers engaged in the chromatographic separation process. Compared to amido coupled fluorenyl phases the slightly increased system mobility of *n*-alkyl fluorenyl phases has a favorable effect on the selectivity for PAHs, since the aromatic ligand fragments play a significant role during the separation process. The three phases with a higher ligand density showed a better selectivity with an improved peak symmetry for PAHs compared to the amido coupled fluorenyl phases. The separations on the latter phase type were performed with an isocratic methanol–water ratio of 85:15 [19], whereas a gradient had to be implemented for the *n*-alkyl fluorenyl phases starting with a more polar mobile phase composition. Especially, the separation of the PAH sets 3/4, 5/6, 7/8, or 11/12 was a problem for stationary phases of the fluorene-I type [5a(T^n)(Q^m)$_y$]. According to Sander et al. [49] C_{18}

phases which are not strongly polymeric are unable to separate sufficiently their critical PAH sets 3/4, 9/10, or 15/16. The critical PAH sets for *n*-alkyl fluorenyl phases are a combination of the above-mentioned PAH sets. None or just partial selectivity was obtained for the PAH set 9/10 with the phase fluorene-10A [4a(T^n)(Q^m)$_y$] and, additionally the PAH set 11/12 in the case of the phases fluorene-6A [3a(T^n)(Q^m)$_y$] and fluorene-10C [4c(M^1)(Q^m)$_y$].

In some cases an increased system mobility of the stationary phase does not automatically result in a better selectivity as demonstrated by the separation of nitro explosives. The less mobile amido coupled fluorenyl phases show better separation capabilities for this task than *n*-alkyl fluorenyl phases [19]. The weak electron pushing effect of the amido group on the fluorene give rise to better π-electron donor properties compared to *n*-alkyl fluorenyl phases. The resulting π-donor–acceptor complexes are responsible for the inverted elution order as compared to *n*-alkyl phases [24]. In the case of *n*-alkyl fluorenyl phases there is an additional interference of the weaker π-electron donor properties of the fluorene fragments with hydrophobic interactions of the alkyl chain fragments. The interference of these opposing separation effects are responsible for the reduced selectivity on nitro explosives.

In analogy to the results of the Sander and Wise test, the length of the *n*-alkyl spacer significantly influences the elution order of nitro explosives. The elution order of the phase fluorene-6A [3a(T^n)(Q^m)$_y$] exhibits the closest similarities to the one of the amido coupled phase fluorene-I [5a(T^n)(Q^m)$_y$]. An increasing number of nitro groups attached to the aromatic solute molecules resulted in an increasing π-acceptor activity and, therefore, longer retention times. The fluorene ligand fragments act as the main interaction center during the separation process due to a short alkyl spacer length in combination with a high ligand density. It is remarkable that the same elution order is observed for the phase fluorene-6B [3b(T^n)(Q^m)$_y$], although it has a much lower ligand density. Thus, the fluorene fragments are not packed very closely and a solute molecule should interact much easier with the alkyl chain fragments indicated by a different elution order. But there is no indication of a strong involvement of the alkyl spacer fragments into the separation process. The observed elution order proves the predominance of π–π interactions for *n*-hexyl fluorenyl phases. In the case of the phase fluorene-10A [4a(T^n)(Q^m)$_y$] the alkyl chain becomes more strongly involved in the separation process due to an increased spacer length. The ligand density of the monofunctional phase fluorene-10C [4c(M^1)(Q^m)$_y$] is much lower as compared to fluorene-10A [4a(T^n)(Q^m)$_y$]. Therefore, the alkyl spacer fragments become much more easily accessible to the solute molecules and they function as the main interaction center during the separation process. The elution order of the monofunctional phase fluorene-10C [4c(M^1)(Q^m)$_y$] closely resembles that of the C_{18} phases, trinitro compounds are eluted prior to dinitro or mononitro compounds. The drastic differences in the elution order of the nitro explosives, as shown in Fig. 13, are proof that *n*-alkyl fluorenyl phases can be classified as mixed-mode phases. Depending on the length of the *n*-alkyl spacer and the density of the attached fluorenyl ligand fragments, either hydrophobic or π–π interactions dominate the interaction mechanism during the separation process.

By consideration of the results obtained from both, solid-state NMR spectroscopy and HPLC applications the following conclusion about *n*-alkyl fluorenyl phases can be made. An improved system mobility in combination with a high ligand density has a favorable effect on the selectivity for PAH samples. Useful chromatographic behavior is obtained by the application of *n*-alkyl fluorenyl phases synthesized with chlorosilanes, because the respective stationary phases possess a sufficient amount of interaction centers engaged in the separation process. The influence of the length of the *n*-alkyl spacer on the separation process was demonstrated by the separation of nitro explosives. A predominance of π–π interactions and the fluorenyl ligand fragment acting as the main interaction center can just be observed in the case of *n*-hexyl fluorenyl phases. In the case of the *n*-decyl fluorenyl phases the involvement of the *n*-alkyl spacer in the separation process is getting stronger, especially for phases with a lower ligand density. The improved accessibility of the *n*-decyl spacer fragments results in an inversion of the elution order of nitro explosives in comparison to phases with a *n*-hexyl spacer. This dependance on the *n*-alkyl spacer length (hydrophobic interactions)

and the ligand density of the fluorene ($\pi-\pi$ interactions) demonstrates the classification of the investigated *n*-alkyl fluorenyl phases as mixed-mode phases in an impressive manner. Their properties with respect to their separation behavior and their system mobility are between the properties of amido coupled fluorenyl phases on the one hand and conventional *n*-alkyl phases on the other hand.

Acknowledgements

We wish to thank Dr. Lane C. Sander (NIST, Gaithersburg, USA) for the donation of the SRM 1647 test mixture and Bischoff Analysentechnik und -geräte GmbH (Leonberg, Germany) for providing silica gel. Ingo Schnell (research group of Professor Dr. H.W. Spiess, MPI Mainz, Germany) and Martin Raitza are thanked for helpful discussions concerning performing the dipolar filter solid-state NMR measurements. Financial support by the Deutsche Forschungsgemeinschaft (Forschergruppe, grant No. Li 154/41-3) is gratefully acknowledged.

References

[1] K.K. Unger, Packings and Stationary Phases in Chromatographic Techniques, Chromatographic Science Series, Vol. 47, Marcel Dekker, New York, Basel, 1990.
[2] L.C. Sander, S.A. Wise, in: R.M. Smith (Ed.), Retention and Selectivity in Liquid Chromatography, Journal of Chromatography Library, Vol. 57, Elsevier, Amsterdam, 1995, p. 337.
[3] W. Hesselink, R. Schiffer, P.R. Kootstra, J. Chromatogr. A 697 (1995) 165.
[4] M. Pursch, L. Sander, K. Albert, Anal Chem. 68 (1996) 4107.
[5] M. Pursch, R. Brindle, A. Ellwanger, L.C. Sander, C.M. Bell, H. Händel, K. Albert, Solid-State NMR 9 (1997) 191.
[6] M. Pursch, S. Strohschein, H. Händel, K. Albert, Anal. Chem. 68 (1996) 386.
[7] S. Strohschein, M. Pursch, H. Händel, K. Albert, Fresen. J. Anal. Chem. 357 (1997) 498.
[8] L.C. Sander, K.E. Sharpless, N.E. Craft, S.A. Wise, Anal. Chem. 66 (1994) 1667.
[9] S. Strohschein, G. Schlotterbeck, J. Richter, M. Pursch, L.-H. Tseng, H. Händel, K. Albert, J. Chromatogr. A 765 (1997) 207.
[10] S. Strohschein, M. Pursch, D. Lubda, K. Albert, Anal. Chem. 70 (1998) 13.
[11] M. Pursch, L.C. Sander, H.-J. Egelhaaf, M. Raitza, S.A. Wise, D. Oelkrug, K. Albert, J. Am. Chem. Soc. 121 (1999) 3201.
[12] F. Mikes, G. Boshart, E. Gil-Av, J. Chem. Soc., Chem. Commun (1976) 99.
[13] F. Mikes, G. Boshart, E. Gil-Av, J. Chromatogr. 122 (1976) 205.
[14] N. Tanaka, Y. Tokuda, K. Iwaguchi, M. Araki, J. Chromatogr. 239 (1982) 761.
[15] C.H. Lochmüller, M.L. Hunnicutt, R.W. Beaver, J. Chromatogr. Sci. 21 (1983) 444.
[16] M. Verzele, N. van de Velde, Chromatographia 20 (1985) 239.
[17] M. Diack, R.N. Compton, G. Guiochon, J. Chromatogr. 639 (1993) 129.
[18] M. Funk, H. Frank, F. Oesch, K.L. Platt, J. Chromatogr. A 659 (1994) 57.
[19] R. Brindle, K. Albert, J. Chromatogr. A 757 (1997) 3.
[20] A. Ellwanger, R. Brindle, K. Albert, J. High Resolut. Chromatogr. 20 (1997) 39.
[21] J.G. Dorsey, K.A. Dill, Chem. Rev. 89 (1989) 331.
[22] H. Hemetsberger, in: K.K. Unger (Ed.), Packings and Stationary Phases in Chromatographic Techniques, Chromatographic Science Series, Vol. 47, Marcel Dekker, New York, Basel, 1990, p. 511.
[23] A. Tchapla, S. Heron, E. Lesellier, H. Colin, J. Chromatogr. A 656 (1993) 81.
[24] E.S.P. Bouvier, S.A. Oehrle, LC·GC Int. 8 (1995) 338.
[25] W. Wielandt, A. Ellwanger, K. Albert, E. Lindner, J. Chromatogr. A 805 (1998) 71.
[26] K. Albert, A. Ellwanger, M. Dachtler, T. Lacker, S. Strohschein, J. Wegmann, M. Pursch, M. Raitza, in J. Blitz, C. Little (Eds.), Fundamentals and Applied Aspects of Chemically Modified Surfaces, Vol. 7, The Royal Society of Chemistry, Cambridge, 1999, p. 111.
[27] H.-J. Egelhaaf, D. Oelkrug, A. Ellwanger, K. Albert, J. High Resolut. Chromatogr. 21 (1998) 11.
[28] L.C. Sander, J. Chromatogr. Sci. 26 (1988) 380.
[29] L.C. Sander, S.A. Wise, LC·GC Int. 3 (1990) 24.
[30] C.A. Fyfe, Solid State NMR for Chemists, C.F.C. Press, Guelph, Ontario, 1983.
[31] G.E. Maciel, D.W. Sindorf, J. Am. Chem. Soc. 102 (1980) 7606.
[32] R. Voelkel, Angew. Chem., Int. Ed. Engl. 27 (1988) 1468.
[33] K. Schmidt-Rohr, H.W. Spiess, Multidimensional Solid-State NMR and Polymers, Academic Press, London, 1994.
[34] M. Goldman, L. Shen, Phys. Rev. 144 (1961) 321.
[35] K. Schmidt-Rohr, J. Clauss, H.W. Spiess, Macromolecules 25 (1992) 3273.
[36] K. Albert, T. Lacker, M. Raitza, M. Pursch, H.-J. Egelhaaf, D. Oelkrug, Angew. Chem., Int. Ed. Engl. 37 (1998) 778.
[37] J. Clauss, K. Schmidt-Rohr, A. Adam, C. Boeffel, H.W. Spiess, Macromolecules 25 (1992) 5208.
[38] J. Clauss, K. Schmidt-Rohr, H.W. Spiess, Acta Polymer. 44 (1993) 1.
[39] E. Bayer, K. Albert, J. Reiners, M. Nieder, D. Müller, J. Chromatogr. 264 (1983) 197.

[40] K. Albert, E. Bayer, J. Chromatogr. 544 (1991) 345.
[41] S.F. Dec, C.E. Bronnimann, R.A. Wind, G.E. Maciel, J. Magn. Reson. 82 (1989) 454.
[42] R. Brindle, M. Pursch, K. Albert, Solid-State NMR 6 (1996) 251.
[43] J.J. Pesek, M.T. Matyska, J. Ramakrishnan, Chromatographia 44 (1997) 538.
[44] M. Pursch, A. Jäger, T. Schneller, R. Brindle, K. Albert, E. Lindner, Chem. Mater. 8 (1996) 1245.
[45] R.L. Silvestri, J.L. Koenig, Macromolecules 25 (1992) 2341.
[46] J. Schaefer, E.O. Steijskal, J. Am. Chem. Soc. 98 (1976) 1031.
[47] J. Schaefer, E.O. Steijskal, R. Buchdahl, Macromolecules 10 (1976) 384.
[48] L.C. Sander, S.A. Wise, J. Chromatogr. A 656 (1993) 335.
[49] L.C. Sander, S.A. Wise, Anal. Chem. 56 (1984) 504.